A Geodesic GIS

Approach to Landing Site Selection for a Human Mission to Mars

Jelmer H.P. Oosthoek[1], Pablo Arriazu[2], Ramiro Marco Figuera[1]

1 Department of Physics and Earth Sciences, Jacobs University, Bremen, Germany
2 Aula Espazio Gela, University of the Basque Country, Bilbao, Spain

Contact email: j.oosthoek@jacobs-university.de

Introduction

The stakes are high when it comes to sending humans to Mars. The scientific results of all past robotic missions need to be incorporated in to making the best selection of a landing site. It would therefore be helpful to encourage publishing data as open source. Geographical information system (GIS) software is a great tool to perform such spatial data analysis and can greatly reduce the number of potential landing sites (1).

Until recently, spatial analysis in a GIS was limited to 2D map projections. These projections are sufficient for local to regional scale studies. However, global scale spatial analyses, such as landing site selection, immediately show the limitations of 2D projections: -180°E equals 180°E. Therefore, a GIS is needed that projects the data on a sphere (or ellipsoid) and that can perform geodesic spatial analysis.

We present the preliminary results of a geodesic-GIS approach to aid the selection of a suitable landing site for a human mission to Mars. The goal is to allow for the selection of 100km radius Exploration Zones (EZs) with the most favorable science and resource Regions of Interest (ROIs).

Methodology

Where not to land humans on Mars. The workshop conveners provided the characteristics of the regions excluded from landing site selection. These data were used to create a GIS dataset (see 'where not to land' in Figure 1). Table 1 shows the data and thresholds used in this step (2-7). As a first estimate, the roughness and dust thresholds were determined through visual inspection of the data histogram and therefore need to be further refined.

Dataset	Threshold	Reference
Mars Orbiter Laser Altimeter	• elevation < 2000 meter • slope < 10 deg	(2)
Robbins Crater Database (> 1km diameter)	> 6 km in diameter = rounding up the diameter of a 25km² circle	(3)
Mars Km-scale Roughness maps	• 0.6 km baseline < 255 • 2.4 km baseline < 255 • 9.2 km baseline < 255	(4)
Mars Global Digital Dune Database		(5)
Dust: Thermal inertia	> 100	(6)
Dust: Albedo	< -8000	(7)

Table 1. *Data used to classify where not to land on Mars.*

Geodesic Buffer approach (using ESRI ArcGIS 10.2). 10 types of potential regions of interest (ROIs) were selected as input (5, 8-16). For each ROI we created geodesic polygon buffers of 100 km (17). We used a 3396.19 km spherical representation of Mars. The buffer method only works with point data. Lines and polygons were first converted to their vertex points (using: 18). The olivine data (16) was provided as a raster dataset and was first converted to a shapefile. The 10 geodesic buffers were combined into one dataset using the ArcGIS Union tool (19). For each ROI, the result contains a field that is set to either 0 (meaning that there is overlap) or -1 (meaning that there is no overlap).

Geodesic Grid approach (using ESRI ArcGIS 10.3). To classify each potential landing site we created a geodesic grid of points, using Matlab and the Delaunay triangulation method (20, 21). The points have been added to a File Geodatabase. Each point approximately reflects a 25 km² circle (the area of the landing site as provided by the workshop conveners). The Generate Near Table tool (22) was used to count the amount of ROIs within 100km distance of each landing site. Point ROIs were simply counted. For line ROIs the length within each EZ was used as a measure. Lines were first simplified using the Simplify Line tool (23) and a 500m tolerance, then split into individual line segments using the ArcGIS Split Line At Vertices tool (24). For each segment the geodetic length was calculated (using: 18). For polygon ROIs see **Future Work**.

Geodesic Buffer approach

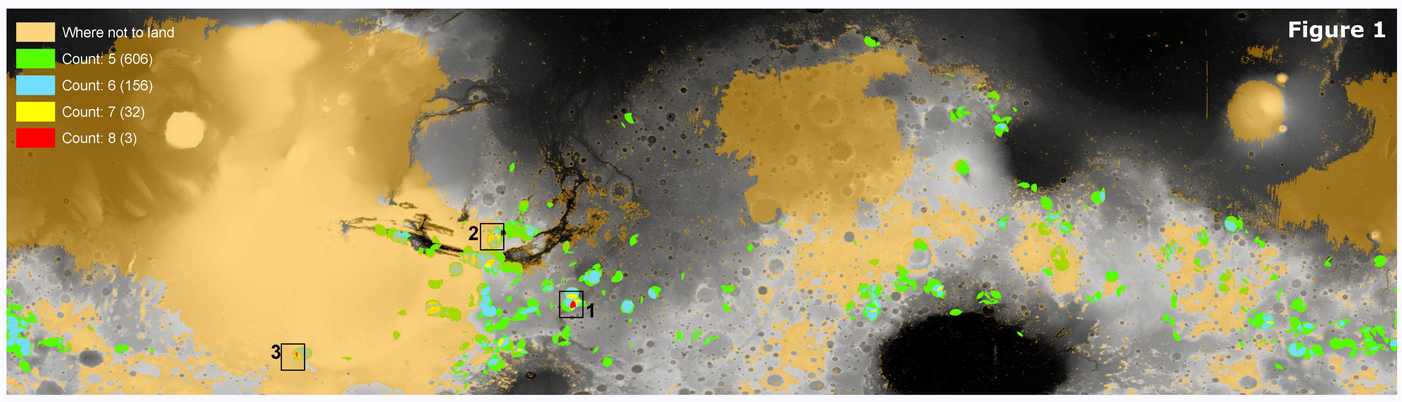

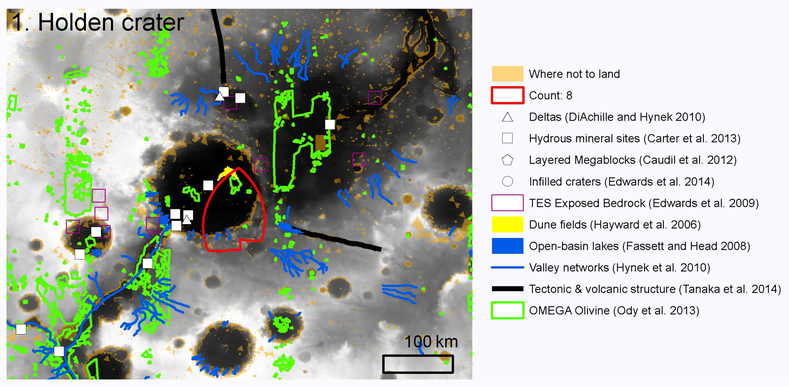

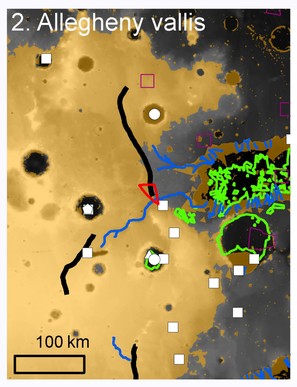

Three areas were found to cover a maximum of 8 out of the 10 geodesic buffers (Figure 1). In other words, 8 of the ROIs are within 100 km distance to these areas. Of these three areas, Holden crater, a Mars Science Laboratory (MSL) candidate landing site (25), proved to be the most promising. The other areas are mostly within the regions excluded from landing site selection.

Besides Holden crater also Eberswalde crater, 30 km north of Holden, falls within 100 km of our resulting area. Both craters contain deltaic deposits (8) and were in the top 4 of candidate landing sites for MSL (25). Holden, Eberswalde and the surrounding region are relatively well covered by high resolution imagery (HiRISE (26)) and hyperspectral data (CRISM (27)) (Figure 2). These datasets have led to the detection of 3 (9-11) of the 10 ROIs. Potential targets, classified using our approach, are therefore expected to lie in the high density areas as seen in Figure 2.

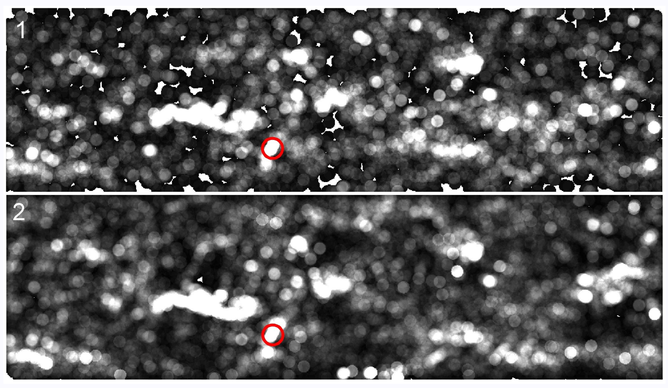

Figure 2. *Density maps of HiRISE (top) and CRISM (bottom) data coverage, between -180° E, 180°E and within 50° N and 50°S. White is high density. The red circle is the location of Holden. The density maps were made using the Point Density tool (28) and CRISM and HiRISE footprint center coordinates.*

Geodesic Grid approach (preliminary)

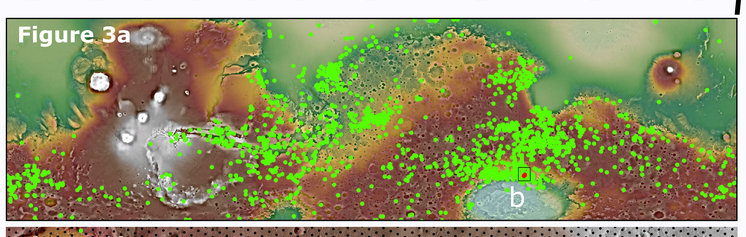

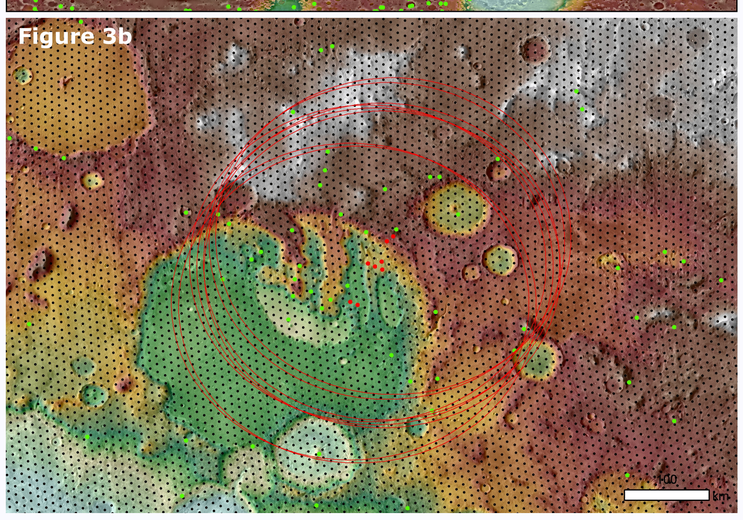

Point ROIs. The green points in Figure 3a and b are the hydrous mineral ROIs (9). Figure 3b shows part of the northern rim of the Hellas basin. The black points are the geodesic grid points. Of these, the red points are 8 geodesic grid points (e.g. possible landing site locations) that have the maximum of 32 hydrous mineral locations within their respective EZs (red ellipses).

Linear ROIs. The blue lines in Figure 4a and b are the valley network ROIs (14). Figure 4b shows the region surrounding Warrego Valles in Thaumasia Planum. In red are eight possible landing site locations with more than 5000 km of total valley network length within their respective EZs. Please note that the 8 EZs lie in the 'where not to land' area (Figure 1).

Discussion. The geodesic grid approach will result in a global database of possible landing site locations. The ROI measurements per geodesic grid point (using simple counting for point ROIs and determining the total length for linear ROIs) can subsequently be used as inputs for a knowledge-driven approach where ROIs are weighted according to their respective importance. This approach could inlude the various criteria shown in the Exploration Zone Rubric (provided by the workshop conveners (29)). These, however, first need to be translated into threshold values.

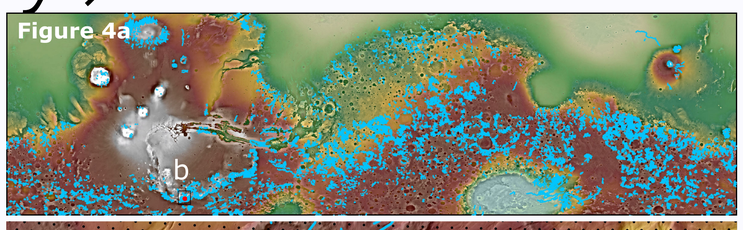

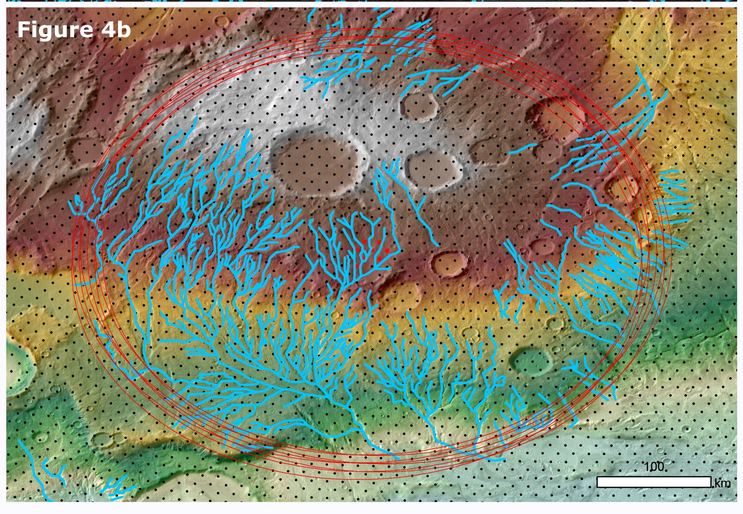

Future Work

Advancing the Geodesic Grid approach. The Geodesic Grid approach will be further advanced. The next step is to include the ability to measure the total area of polygon ROIs (for example olivine deposits (16)) within each possible EZ. We will create a new geodesic point grid, with each point representing 10 km² (or another suitable, to be determined value). The points overlapping the polygon layer will be used with the Generate Near Table tool. The resulting count per EZ will be multiplied by the 10 km² area. This allows for the estimation of the total area of a polygon ROI within each EZ.

A use case application. The approach could be applied within a scientific use case to verify the candidate landing sites for the Mars 2020 (30) rover mission. The Mars 2020 rover has different landing site characteristics (e.g. engineering constraints and landing site ellipses) than a human mission to Mars. Therefore a new geodesic grid based on the Mars 2020 landing site ellipse (16km by 14km) needs to be generated. Instead of the 100 km EZ the expected range of the rover will be used. This will be at least 20 km, the drive capability of MSL Curiosity (31), on which the Mars 2020 rover is based.

References

(1) Koenders R. et al. (2007) http://www.rssd.esa.int/SYS/docs/ll_transfers/1118565.pdf **(2)** Smith D.E. et al. (1999) doi:10.1126/science.284.5419.1495 **(3)** Robbins S.J. and Hynek B.M. (2012) doi:10.1029/2011JE003966 **(4)** Kreslavsky M.A. and Head J.W. (2000) doi:10.1029/2000JE001259 **(5)** Hayward R.K. et al. (2007) http://pubs.usgs.gov/of/2007/1158/ **(6)** Putzig N. and Mellon M. (2007) doi:10.1016/j.icarus.2007.05.013 **(7)** Ody A. et al. (2012) doi:10.1029/2012JE004117 **(8)** Di Achille G. and Hynek B.M. (2010) doi.org/bx7tbd **(9)** Carter J. et al. (2013) doi.org/7mh **(10)** Caudil C.M. et al. (2012) doi.org/7mg **(11)** Edwards C.S. et al. (2014) doi.org/pd2 **(12)** Edwards C.S. et al. (2009) doi.org/bsg47v **(13)** Fassett C.I. and Head J.W. (2008) doi.org/cpdwxs **(14)** Hynek B.M. et al. (2010) doi.org/db5sr6 **(15)** Tanaka K.L. et al. (2014) pubs.usgs.gov/sim/3292/ **(16)** Ody A. et al. (2013) doi.org/7mj **(17)** ESRI (2012) How Buffer (Analysis) works, http://goo.gl/KGBHQq **(18)** Jenness J. (2012) http://www.jennessent.com/arcgis/shapes_graphics.htm **(19)** ESRI (2014) Union, goo.gl/2LTsoj **(20)** Burkardt J. (2012) peo-ple.sc.fsu.edu/~jburkardt/m_src/sphere_delaunay/sphere_delaunay.html **(21)** Oosthoek J.H.P. et al. (2014) 44th LPSC, Abstract #2565 **(22)** ESRI (2014) Generate Near Table, http://goo.gl/0xorFO **(23)** ESRI (2012) Simplify Line, http://goo.gl/SeV57z **(24)** ESRI (2015), Split Line At Vertices, http://goo.gl/Iyl5Jt **(25)** Golombek M. (2012) doi.org/7mk **(26)** McEwen et al. (2007) doi.org/dnd8j3 **(27)** Murchie et al. (2007) doi.org/bksb23 **(28)** ESRI (2014) Point Density, http://goo.gl/TP51q9 **(29)** Human Landing Sites Study Steering Committee, http://www.hou.usra.edu/meetings/explorationzone2015/Matrix_Example.pdf **(30)** Golombek .P. et al. (2015) 46th LPSC, Abstract #1653 **(31)** Grotzinger J.P. et al. (2012). doi:10.1007/s11214-012-9892-2